Title
Interaction Between Spire and Rab GTPases and its Effect on the Developing Drosophila Oocyte

Author
Wang, Liujie

Publication Date
2017

Peer reviewed|Thesis/dissertation

UNIVERSITY OF CALIFORNIA

Los Angeles

Interaction Between Spire and Rab GTPases and its Effect on the Developing *Drosophila* Oocyte

A thesis submitted in partial satisfaction

of the requirements for the degree Master of Science

in Biochemistry, Molecular and Structural Biology

by

Liujie Wang

2017

ABSTRACT OF THE THESIS

Interaction Between Spire and Rab GTPases

and its Effect on the

Developing *Drosophila* Oocyte

by

Liujie Wang

Master of Science in Biochemistry, Molecular and Structural Biology

University of California, Los Angeles, 2017

Professor Margot Elizabeth Quinlan, Chair

Spire, an actin nucleator, is critical for proper oocyte development in *D. melanogaster* via the establishment of an actin mesh network. Knowledge of its interaction with *Drosophila* Rab GTPases, a group of master regulators of membrane trafficking dynamics, would contribute to our understanding of Spire's role in the developing oocyte. *Drosophila* Spire has a putative Rab-binding sequence, the Spir-box, located in the C-terminal half of the protein. Flies lacking the Spir-box have about a 50% decrease in fertility, which supports the idea that the interaction between *Drosophila* Spire and *Drosophila* Rabs is functionally significant. However, the specific Rab(s) involved in the interaction remains unknown. Thus, we set out to identify which specific *Drosophila* Rabs interact with *Drosophila* Spire and whether it is through direct or indirect interactions. Based on previous data showing binding interaction between

mammalian Spire1 and mammalian Rabs 6 and 11 as well as *Drosophila* Rab expression patterns in the oocyte, we chose to start with *Drosophila* Rabs 5, 6, and 11. However, we did not detect a direct interaction in GST pulldown assays with GST tagged Rab 5, 6 and 11 and C-terminal constructs of Spire. This raises the possibility of indirect interactions or the requirement of additional components to stabilize the complex of *Drosophila* Rab(s) and *Drosophila* Spire. Co-IP experiments from ovary lysate will be performed to probe for indirect binding between Spire and Rab 5, 6, and 11. Once specific Rabs have been identified, the complex will be further characterized biochemically with the long-term goal of modifying the binding sites in vitro and determining the functional consequences of these changes in vivo.

The thesis of Liujie Wang is approved.

Albert J. Courey

Frank A. Laski

Emil Reisler

Margot Elizabeth Quinlan, Committee Chair

University of California, Los Angeles

2017

Table of Contents

Acknowledgement

I want to thank the Quinlan lab in particular Dr. Quinlan and Dr. Silkworth for their guidance and support throughout my tenure in the lab. I also want to thank Dr. Reisler, Dr. Laski, and Dr. Courey for their time serving on my thesis committee.

Chapter One: Introduction

1.1 Overview

Proper oocyte development is critical for the overall viability of the *Drosophila* fruit fly, necessary for progression from a fertilized egg into a mature adult. For this to occur, several key developmental milestones must be met; e.g. infusion of nurse cell cytoplasm into the oocyte, localization of polarity markers, and the subsequent positioning of the body axes. The establishment of an actin mesh by Cappuccino and Spire, two actin nucleators, from stage 5 to mid-stage 10 in oocyte development is intimately related to the proper localization of polarity markers through transport on the microtubule (MT) cytoskeleton. The mechanism by which the actin mesh contributes to the organization of the MT network for the specific localization of bicoid, oskar, and gurken mRNA and/or whether the actin mesh directly contributes to polarization are still unclear. However, a Spire-dependent actin mesh is essential for mammalian oogenesis. Thus, a better understanding of both the mesh and Spire's role will contribute to our understanding of cell polarity during early development.

A potential interaction between *Drosophila* Spire and Rab GTPases is intriguing in the context of polarity establishment. Rab GTPases are key regulators of membrane trafficking dynamics, and often implicated in cell polarity. They mediate vesicle movement on both the actin and microtubule networks. Spire contains a putative Rab-binding sequence. Recently, an indirect interaction between mammalian Spire1 and Rab11 was demonstrated (Pylypenko et al., 2016). However, an interaction between *Drosophila* Spire and Rab GTPases has not been observed. We want to understand whether there exists a functional significance for the interaction between Spire and Rab and how it contributes to the overall developmental program of the oocyte.

1.2 Background

To determine whether Spire and Rabs interact directly, we performed in vitro pulldown assays with recombinantly expressed and purified Spire and Rabs. The Spire construct used was ita C-terminal half, which includes the proposed Rab binding domain, called the Spir-box. The Spir-box was identified based on homology to other sequences that have been shown to bind to Rabs. If we find a direct interaction, we can better interpret and analyze the flies deficient in wildtype Spire that express a Spire construct lacking the Spir-box domain.

Spire belongs to the group of WH2 nucleators and binds actin monomers via its WH2 domains to accelerate the formation of filamentous actin. Furthermore, Spire is necessary for proper oogenesis and polarity establishment within the developing *Drosophila* oocyte. The Rab protein family is a group of GTPases that switch between the GDP inactive form and the GTP active form. They regulate various steps of membrane traffic along both actin and microtubule networks.

There are several lines of evidence of an interaction between Spire and Rabs. For example, Rabphilin-3A, a mammalian protein binds Rab3A. The Rab-binding region of Rabphilin-3A shares sequence homology with the Spir-box domain of both *Drosophila* Spire and mammalian Spire1 and Spire2. The Spir-box domain is in the C-terminus of Spire (Fig. 1). The red highlighted residues in Rabphilin-3A directly bind Rab3A and share sequence similarity with the orange aligned residues within the Spir-box region of *Drosophila* Spire and mammalian Spire1 and Spire2.

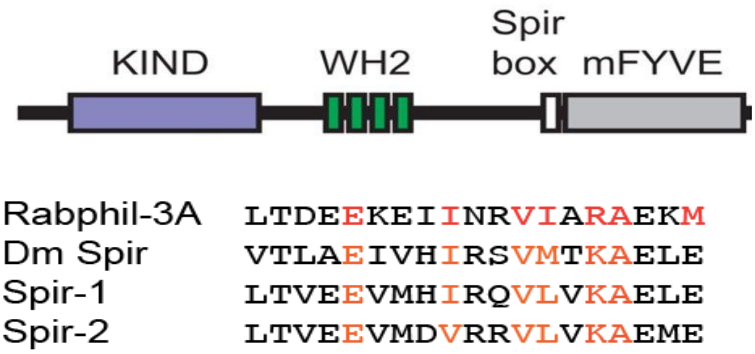

Figure 1: The full-length construct of *Drosophila* Spire with its four major domains; KIND (Capu-binding domain), WH2 (actin binding domain), mFYVE (membrane associated domain), and Spir-box (possible Rab-binding domain). The alignment data shows sequence homology between the Rab-binding domain of Rabphilin-3A and Spire from *Drosophila* and human. The red residues in Rabphil-3A make direct contact with Rab3A.

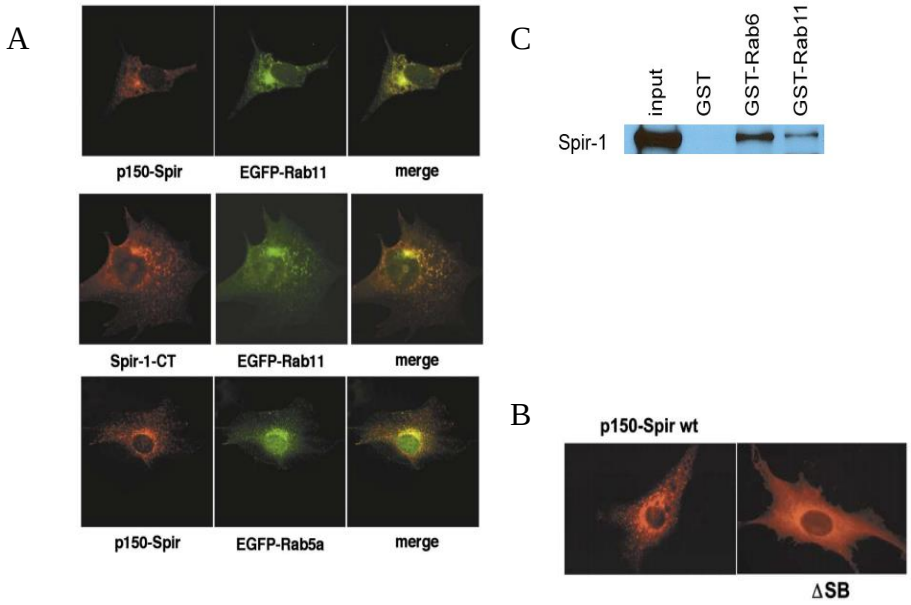

Figure 2: A.) Co-localization of *Drosophila* Spire(p150-Spir) and mammalian Spire1(Spir-1-CT) with Rab11 and none with Rab5. B.) The localization pattern is affected when Spir-box is deleted as shown in the bottom right. C.) The western blot shows pulldown of GFP-Spire1 from HEK293 cells using GST-Rab6 and GST-Rab11. (A and B from Kerkhoff et al., 2001; C our unpublished data)

Previous data also show co-localization between Spire and Rab11, while the localization pattern of *Drosophila* Spire is affected when the Spir-box domain is deleted (Fig. 2A,B; Kerkhoff et al., 2001). The merge data display similar localization patterns between Rab11 with both mammalian(Spir-1-CT) and *Drosophila* Spire(p150-Spir). However, co-localization between *Drosophila* Spire and Rab5a is absent in the merge data. GST-Rab pulldowns from HEK293 cells expressing GFP-Spire1 show its interaction with Rab6 and Rab11 (Fig. 2C). Recombinantly expressed and purified GST-Rab6 and GST-Rab11 were incubated with HEK293 cell lysate and subsequently probed for Spir-1 using a Spir-1 specific antibody in a western blot. This suggests that Rabs function as trafficking signals for Spire's localization. This effect could be magnified in the oocyte where Spire mis-localization could disturb actin mesh formation and polarity establishment.

Thus, knowing that Spire is involved with actin dynamics, we want to further investigate the interaction between Spire and Rab in order to uncover any possible role that Spire has in membrane trafficking dynamics within the context of *Drosophila* oocyte development. Given the previous data showing interactions of Spire1 with Rab6 and Rab11, as well as no co-localization of *Drosophila* Spire with Rab5, we chose to start our investigation with *Drosophila* Rab6, Rab11 and using Rab5 as a negative control to assess these interactions.

Our main goals include the following:

- Improve the solubility of the C-terminal fragment of *Drosophila* Spire
- Express and purify GST tagged *Drosophila* Rab5, Rab6 and Rab11
- Test for direct interaction between Spire and Rab5, 6, and 11
- Test for indirect interaction between Spire and Rab5, 6 and 11
- Assess the functional significance of the Spir-box domain in the context of the developing *Drosophila* oocyte.

1.3 Literature Overview

1.3a *Drosophila* Oocyte

Positioned at the posterior of the egg chamber, the oocyte consists of a group of 16 interconnected germ cells surrounded by a layer of somatic follicle cells. During formation of the egg chamber, one of the germ cells becomes the oocyte while the rest develop into nurse cells. In subsequent axis orientation, bicoid, oskar and gurken mRNAs, which determine the embryonic axes, localize to the anterior, posterior, and anterodorsal poles of the oocyte respectively (Riechmann and Ephrussi, 2001).

1.3b Actin Cytoskeleton

The actin cytoskeleton and its dynamic growth play an integral part in many cellular functions, including but not limited to motility, vesicle trafficking, and signaling. The assembly and disassembly of actin filaments from its globular components need to be coordinated with a particular cellular function in order to properly carry out the process. Actin filaments grow in a polarized fashion through the addition of ATP-actin monomers to the barbed or fast-growing end of the filament. Simultaneously, as the ATP hydrolyzes, filamentous ADP-actin is disassembled and removed from the pointed or slow growing end of the filament. This cycle is regulated by actin binding proteins. Of great interest is the nucleation step, which is the rate-limiting step in actin filament formation. It is controlled and accelerated by three nucleation factors (Pollard et al., 2003). These include the Arp2/3 complex, the Formin protein family and the WH2 nucleators.

The Arp2/3 complex stimulates actin filament formation through the action of its two actin like subunits, Arp2 and Arp3. Upon complex binding to the side of a pre-existing filament, Arp2 and Arp3 mimic the barbed end of a new actin filament enabling monomer addition. This allows for the generation of branched filament structures (Pollard et al., 2003). The formins catalyze actin filament formation

through dimerization to form a hoop shaped structure that acts like a barbed end cap. Formins allow ATP-actin monomers to insert between the cap and the barbed end of actin filaments (Xu et al., 2004). The exact mechanism of this process has not been fully elucidated. The focus here will be on *Drosophila* Spire, which belongs to the group of WH2 nucleators. Spire nucleates actin filaments by binding actin monomers through its four tandem WH2 domains and positioning the actin monomers into a nucleation center for further addition of actin.

1.3c *Drosophila* Spire

The *spire* gene was initially identified along with *cappuccino*, a *Drosophila* formin, in a screen for mutations affecting polarity in *Drosophila* oocytes (Manseau et al., 1989). A conserved metazoan protein, *Drosophila* Spire contains several notable domains within its sequence. It has multiple copies of the WH2 motif, a well-characterized actin-binding domain (Wellington et al., 1999). WH2-like motifs are present in a wide range of actin binding proteins (Paunola et al., 2002) with two distinct subclasses: those related to a region in the Arp2/3 activator WASp and the others which share closer similarity to actin monomer sequestering protein, thymosin B4. Spire WH2 domain falls into the WASp category and was hypothesized to be an Arp2/3 activator. Subsequent test of the activity of Spire WH2 domains in an actin polymerization assay showed promotion of actin filament formation in the absence of the Arp2/3 complex (Quinlan et al., 2005). Thus, Spire represented a novel class of actin nucleators in addition to the Arp2/3 complex and the Formin protein family.

Apart from the four WH2 repeats in the amino terminus of Spire, the KIND domain, which is N-terminal to the WH2 repeats, functions to bind and regulate the actin-nucleating activity of Cappuccino (Capu), a *Drosophila* formin, as well as bind intra-molecularly to its own C-terminal half (Quinlan et al., 2007, Vizcarra et al., 2011; Tittel et al., 2015). Both Spire and Capu are required for the correct formation and maintenance of an actin mesh in the developing *Drosophila* oocyte. This actin mesh spans the

Drosophila oocyte during mid-oogenesis and its absence correlates with rapid microtubule-dependent cytoplasmic streaming (Dahlgaard et al., 2007). Furthermore, mutations in either Capu or Spire disrupt proper axis formation in the oocyte and cause female sterility (Manseau and Schupbach, 1989). The C-terminal half of Spire contains two important domains, namely the Spir-box and the mFYVE domain. The latter is highly homologous to FYVE motifs and localizes onto the membrane through a zinc finger structure (Otto et al., 2000; Tittel et al., 2015). The former is of particular interest due to previous work showing Rab GTPase binding interaction with a conserved region much like the Spir-box sequence between Rab3A and Rabphilin-3A. (Kerkhoff et al., 2001). Rabphilin-3A is a mammalian protein effector that binds human Rab3A through its Rab-binding domain. The significance of this is that since the Spir-box domain of *Drosophila* Spire and human Spire1 and Spire2 share close sequence homology with the Rab-binding domain, it stands to reason that *Drosophila* could possibly interact with Rab GTPases through its Spir-box.

The Spir-box region is just N-terminal to the mFYVE domain and spans a region of 20 amino acids. It exhibits sequence similarity to the alpha-helical N-terminal extension of the Rabphilin-3A FYVE domain as shown in Fig 1. This FYVE domain mediates the interactions between Rabphilin-3A and the switch regions 1 and 2 of the Rab3A GTPase (Ostermeier et al., 1999). Co-expression of *Drosophila* Spire and GFP tagged Rab GTPases in NIH 3T3 cells results in co-localization between Spire and Rab11. Rab11 is primarily localized to post-Golgi vesicles and endosomes (Sonnichsen et al., 2000). Co-localization of Spire and Rab11 depends on the integrity of the Spir-box and the mFYVE domain (Kerkhoff et al, 2001). This introduces the possible connection between vesicle trafficking and the actin network mediated by the interaction between *Drosophila* Spire and *Drosophila* Rab proteins.

1.3d Rab GTPases and Vesicle trafficking

Vesicle trafficking between compartments is vital for cellular function and intracellular communication. The various processes in trafficking such as vesicle formation, vesicle fusion, tethering and targeting are regulated by members of the Rab family of GTPases (Stenmark, 2009; Pfeffer, 2007; Jordens et al., 2005). GTPases function as molecular switches turning on/off from GTP to GDP bound states respectively. This is particularly important in the release of neurotransmitters in neurons, as this process requires precise control by the membrane trafficking system (Ng et al., 2008; Pavlos et al., 2011).

The first characterized member of the Rab family was a yeast Rab, Ypt1. While related to Ras, Ypt1 does complement the loss of the RAS1 and RAS2 gene in yeast. This suggested that its functional role differs from that of the Ras proteins (Schmitt et al., 1986). Yeast encode 11 Rabs while human cells encode 63 known Rabs (Colicelli, 2004). Most Rabs are C-terminally prenylated on two cysteines, allowing for tight membrane association. Rab5 was initially shown to function as the rate-limiting step for endosome fusion and endocytosis (Gorvel et al., 1991). Rab proteins are trafficked to membranes via the interaction with GDP-dissociation inhibitor (GDI) and occasionally with GDI-displacement factors (GDF). Subsequent interaction with GTP exchange factor (GEF) diminishes Rabs' susceptibility to GDI extraction. This stabilizes Rabs at the site of activation with the help from GTP-dependent effectors. (Aivazian et al., 2006).

Rab proteins recruit motor proteins and tethering factors to facilitate membrane trafficking events leading to polarized secretory and endocytic pathways (Ortiz et al., 2002; Rivera-Molina and Novick, 2009).

The regulation of membrane trafficking is also crucial for patterning and differentiation during the development of multicellular organisms. It guides the development of cell and tissue polarity (Apodaca et al., 2012; Winter et al., 2012) and allows cells to secrete or absorb particular cargo in response to different

signals (Cao et al., 2012). A study by Dunst et al, 2015 showed that a core group of Rabs (1,5,6,7,11), which has been maintained in almost all eukaryotes, organizes the basic membrane trafficking machinery common to all cells while other Rabs tend to have tissue-specific functions.

1.3e *Drosophila* Rab GTPases

The *Drosophila* genome includes 31 Rab or Rab-like genes, the majority of which have orthologs to the 75 vertebrate Rabs (Zhang et al., 2007). Work characterizing *Drosophila* Rab proteins supports a strong conservation of Rab localization and function between flies and mammals (Zhang et al., 2007; DiAntonio et al., 1993; Wucherpfennig et al., 2003; Emery et al., 2005; Satoh et al., 2005). The expression patterns of 25 rab loci show that about half of the Rabs are expressed either predominantly or exclusively in neurons (Chan et al., 2011) while the other Rabs are expressed in a variety of neuronal and non-neuronal cell types, including the common endosomal compartment markers such as Rab5 and Rab11.

1.3f *Drosophila* Rab5 in oocyte

Assembly of the *Drosophila* axes begins with the localization and translation of *oskar* RNA at the oocyte posterior pole. There are two isoforms of Osk. Short Osk recruits other pole plasm components while long Osk restricts them to the oocyte cortex. Several vesicular trafficking components, that function downstream of long Osk, have been identified. Among them are the Rab5 effector protein Rabenosyn-5 (Rbsn-5) and the endosomal protein Mon2. Both are critical for Osk-induced actin remodeling (Tanaka and Nakamura, 2011). *Drosophila* Rab 5 is present throughout the oocyte cortex and enriched at the posterior pole (Dollar et al., 2002; Tanaka et al., 2008). In both Rbsn-5 and Drab5 mutant oocytes, the Osk and other pole plasm components failed to be anchored. Ectopically localized Osk did not induce formation of F-actin projections in these backgrounds (Tanaka et al., 2008, 2011). This suggests an

important role of Rbsn5/Rab5 in mediating osk-induced rearrangement of F-actin for anchorage at the oocyte posterior cortex.

1.3g *Drosophila* Rab6 in oocyte

Members of the Rab6 family regulate protein transport between the ER, Golgi, plasma membrane and endosomes (Del Nery et al., 2006; Mallard et al., 2002; Martinez et al., 1997; Opdam et al., 2000). Previously, *Drosophila* Rab6 (Drab6) was shown to be involved in both Rhodopsin transport in photoreceptor cells and bristle morphogenesis (Purcell et al., 1999; Shetty et al., 1998). Drab6 is primarily localized to the Golgi in *Drosophila* oocytes (Januschke et al., 2007). Furthermore, in the oocyte, Drab6 is necessary for the anterodorsal secretion of Gurken. This leads to follicle cell differentiation, which controls the morphogenesis of the dorsal appendages of the egg shell. In the absence of Drab6, Gurken is mis-localized to lysosomal or late endosomal compartments and osk mRNA is incorrectly localized in the oocyte (Januschke et al., 2007). Depletion of Drab6 in the germ line caused membrane-trafficking defects and in turn altered the egg-chamber plasma membrane composition and proper organization of the germline cyst. Lack of Drab6 during mid-oogenesis yielded an abnormally polarized oocyte MT network (Coutelis and Ephrussi, 2007). Furthermore, the nurse cell cortical actin cytoskeleton progressively disappeared from stage 2 to stage 7, in 80 percent of Rab6-null egg chambers (Coutelis and Ephrussi, 2007). This was validated through a complete rescue by a heat inducible Rab6 transgene.

1.3h *Drosophila* Rab11 in oocyte

Drosophila Rab11 (Drab11) is localized to the posterior end of the oocyte. Drab11 mediates receptor recycling, which plays a vital role in the polarization of the oocyte cytoplasm. This polarization functions through specific membrane domains, which support osk mRNA translation and anchoring (Dollar et al., 2002). Drab11 is required for polarized endocytic recycling and for the organization of membrane

compartments at the posterior end of the oocyte (Dollar et al., 2002). Osk is required for preferential localization of Drab11 to the posterior pole. In addition, Drab11 is required for the efficient transport of osk mRNA to the posterior pole of the oocyte and its translation at the posterior pole. This suggests a positive feedback loop for Drab11 and Osk. As some osk mRNA is localized and translated at the posterior pole, Drab11 is recruited and enhances the transport of osk mRNA to the pole that in turn recruits more Drab11 and the cycle continues.

Chapter Two: Materials and Methods

2.1 Experimental Approach

Protein aggregation was a main issue in obtaining soluble SpireCT fraction. Thus, we employed two strategies to try to resolve this problem.

The first involved performing a co-expression of Spire-KIND, residues 1-327, along with SpireCT. Spire has been shown to self-interact through these two portions of its sequence. Thus, the idea was to have SpireCT and KIND interact and keep SpireCT in the folded form, then perform affinity chromatography against the GST tag on SpireCT and His tag on Spire-KIND.

The second strategy involved the removal of a loop sequence within the SpireCT construct. This sequence was thought to affect the folding of SpireCT due to its general flexibility. Through blunt ligation cloning, we deleted the region spanning residues 814 to 949 to generate the new SpireCTΔLoop construct.

For the expression of GST tagged *Drosophila* Rab5, Rab6, and Rab11, we inserted the constructs into pGEX vectors with an N-terminal GST tag, expressed in Rosetta 2 cells and purified with affinity chromatography. We used the purified GST-Rab5, GST-Rab6, and GST-Rab11 for the subsequent pulldown assay with recombinantly expressed SpireCT constructs in cell lysate.

We used the same purified GST-Rab proteins for pulldown of GFP-Spire from fly ovary lysate. Western blots on pulldown samples were performed for analysis of direct or indirect interactions between *Drosophila* Spire and Rab5, Rab6 and Rab11.

Lastly, we will use the MiMIC system to create fly lines expressing Spire deficient in its Spir-box domain.

2.2 Generation of GST-SpireCTΔLoop construct

Forward and reverse DNA primers for the residues flanking the 814-949 region of SpireCT were designed in SnapGene and ordered from IDT. Using these two primers along with SpireCT in a pGEX vector as the template sequence, linearized PCR product lacking the 814-949-sequence region was generated. The linearized PCR product was phosphorylated using T4 Polynucleotide Kinase and then blunt ligated using T4 DNA Ligase to create the pGEX-SpireCTΔLoop construct.

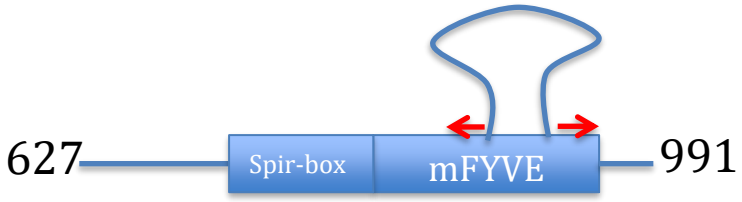

SpireCT in pGEX vector with N-terminal GST

Figure 3: The SpireCT construct is shown with the unstructured loop section depicted. The red arrows flank the 814-949 residues and represent the locations of the forward and reverse DNA primers for the generation of the GST-SpireCTΔLoop construct.

2.3 Generation of His6-SpireCTΔLoop Constructs

Forward and reverse primers with CATCATCAT (3His) overhangs were designed against the start site of SpireCTΔLoop and the start site of the GST tag respectively, using the GST-SpireCTΔLoop as the template. PCR, using these two primers and the GST-SpireCTΔLoop template, generated a linearized product lacking the GST sequence while retaining the 3His residue sequence at its 5 and 3 prime ends. Subsequent phosphorylation via T4 Polynucleotide Kinase and blunt ligation using T4 DNA Ligase yielded a pGEX vector with the SpireCTΔLoop sequence containing an N-terminal His6 tag and devoid of a GST sequence. For the generation of the His6-linker-SpireCTΔLoop construct, the linker sequence

was inserted into the vector between the His6 and the SpireCTΔLoop sequences through restriction-free cloning.

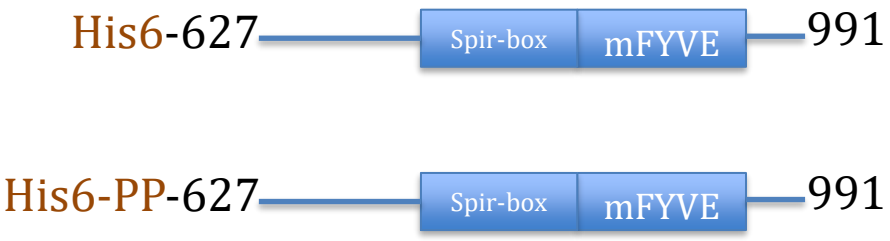

Figure 4: The constructs for His6-SpireCTΔLoop and His6-PP-SpireCTΔLoop are depicted above. Both are in a pGEX vector and the only difference between the two is the introduction of a Prescission Protease linker sequence between the N-terminal His6 tag and the start of the SpireCTΔLoop sequence.

2.4 Generation of GST-Rab5, GST-Rab6, and GST-Rab11

DNA plasmids of Rab5, Rab6, and Rab11 were obtained from the *Drosophila* Genome Resource Center. Forward and reverse primers with BamHI and NotI restriction cut sites were respectively designed for each of the Rab sequences. PCR amplification yielded linear DNA fragments of each Rab containing BamHI cut site and NotI cut site at the 5 prime and 3 prime ends. Each fragment and the pGEX destination vector were digested with BamHI and NotI restriction enzymes. Subsequent ligation of the two pieces using T4 DNA Ligase resulted in the constructs of GST-Rab5, GST-Rab6, and GST-Rab11.

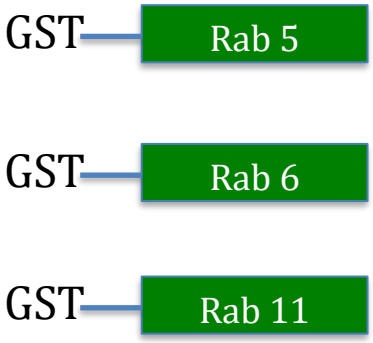

Figure 5: The GST-Rab constructs are shown. Each construct was cloned into a pGEX vector containing an N-terminal Glutathione S-Transferase.

2.5 Expression of Spire and Rab constructs

GST-SpireCTΔLoop, His6-SpireCTΔLoop and His6-linker-SpireCTΔLoop were all individually transformed into Rosetta2 Cells (BL21 derivative). GST-Rab constructs were individually transformed into BL21 cells. These cells were inoculated in starter cultures and grown overnight at 37°C. These starter cultures were inoculated into 1 Liter TB Media at a volume ratio of 1mL of starter culture per 50ml of TB Media along with ampillcin and chloramphenicol. The 1 Liter cultures were shaken at 37°C until around an OD(600) of 0.6 and then induced with 250uM of IPTG and shaken at 18°C for 18 hours. Cell pellets were harvested, flash-frozen and stored at -80°C for later use.

2.6 Purification of Spire and Rab constructs

GST-tagged Protein Purification:

Including GST-SpireCTΔLoop, GST-Rab5, GST-Rab6, GST-Rab11

Cells were resuspended in 1xPBS(140mM NaCl; 2.7mM KCL; 10mM Na_2HPO_4; 1.8mM KH_2PO_4; pH 7.4) and passed through a microfluidizer for lysis and homogenization. Cell lysate was spun down at 20,000g for 20 minutes. A pellet fraction was collected to assess the level of protein aggregation of the GST-SpireCTΔLoop, or GST-Rabs. The supernatant fraction was retained and mixed with Glutathione Sepharose Resin. After binding for 1 hour, the flow-through fraction was collected and then two 1xPBS washes were applied to the resin column. A glutathione elution buffer was then applied to exchange the bound GST-SpireCTΔLoop with glutathione. For each step in the purification, 20ul samples were collected to run on a 10% SDS gel in order to assess the effectiveness of the purification.

His6-tagged Protein Purification:

Including His6-SpireCTΔLoop, His6-linker-SpireCTΔLoop

Cells were resuspended in Talon Extraction Buffer (300mM NaCl, 50mM NaPhosphate, 1mM BME, pH 8.0) and passed through a microfluidizer for lysis and homogenization. Cell lysate was spun down at 20,000g for 20 minutes. A pellet fraction was collected to assess the level of protein aggregation of both His6-SpireCTΔLoop and His6-linker-SpireCTΔLoop. The supernatant fraction was retained and flowed onto Talon Affinity Resin. After binding for 1 hour, the flow-through fraction was collected and then two Talon wash buffer fractions (300mM NaCl, 50mM NaPhosphate, 1mM BME, pH 7.0) were applied to the resin column. An imidazole elution buffer (200mM Imidazole, 300mM NaCl, 50mM NaPhosphate, 1mM BME, pH 7.0) was then applied to exchange the bound His6-SpireCTΔLoop or His6-linker-SpireCTΔLoop with imidazole. For each step in the purification, 20ul samples were collected to run on a 10% SDS gel in order to assess the effectiveness of the purification.

2.7 Co-expression Assay

Colonies from previously co-transformed Rosetta 2 cells for Spire520-991+Spire-KIND and Spire699-991+Spire-KIND were grown in an LB media starter culture for 18 hours. This starter culture was introduced into TB media in a volume ratio of 1:50, i.e. 1ml of starter culture into 50ml of TB media. This new culture was inoculated with ampicllin, chloroamphenicol and kanamycin and then grown to an optical density around 0.5 measured at 600nm. Afterwards, 8ml aliquots of the TB media culture were divided into separate test tubes for assessment of each expression condition. IPTG was then introduced under different conditions specific for each test tube and allowed to grow overnight at 18°C. Cell samples were collected before and after addition of IPTG to assess the relative expression levels of the protein constructs.

This procedure was duplicated for the singly transformed Rosetta 2 cells containing only the respective Spire520-991 and Spire699-991 plasmids. Western blot was performed afterwards to observe expression differences between singly transformed and co-transformed cells.

2.8 Co-Expression of SpireCT constructs with Spire-KIND

Spire-KIND in a pRSF1b vector and Spire520-991 in a pET vector were co-transformed into Rosetta 2 cells. This was also done with Spire-KIND and Spire699-991 in a pET vector. After selecting against ampicllin, chloroamphenicol and kanamycin, these cells were grown in TB media, induced with 250uM IPTG and harvested after 18 hours of induction. Cell pellets were divided into one-gram aliquots and stored at -80°C for subsequent Rab pulldown assay.

2.9 Refolding Assay Protocol

Elution fractions from His6-SpireCTΔLoop and His6-PP-SpireCTΔLoop purification under denaturing conditions were collected individually and subjected to gradient dialysis. The elutions were initially in 8M urea conditions. They were first dialyzed against 1L dialysis buffer (10mM Tris, 50mM KCl, pH 8.0, 1mM DTT) containing 4M urea for 2 hours. Next, they were switched into 1L dialysis buffer containing 2M Urea for 2 hours followed by 1L dialysis buffer with no urea for 2 hours and another 1L of dialysis overnight. After this gradient dialysis, the samples were subjected to a high-speed spin to separate the soluble and insoluble fractions. Gel samples were collected for analysis of the refolding assay attempt.

2.10 GST-Rab Pulldown Assay Protocol

Process Steps for Resin Prep for GST-Rab5, 6, 11

1. Re-suspend beads and take 40ul of 50% slurry and wash with 1.5ml of cold 1xPBS; centrifuge at 1000rpm for 3 minutes.

2. Decant supernatant and repeat 1xPBS wash for 2 additional times (3xtimes 1xPBS).

3. Perform a final wash with dialysis buffer and re-suspend 20ul of GST resin in 180ul of dialysis buffer (50mM KCl, 10mM Tris, pH 8.0) for a total of 200ul (2xtimes dialysis buffer).

4. Add 50ul aliquot of GST-Rab11 into the 200ul GST resin mixture; Rotate for 2 hours at 4 °C.

5. Centrifuge at 1000rpm for 3 minutes and remove supernatant; wash GST-Rab11 bound resin with dialysis buffer; repeat for 2 additional times.

6. Re-suspend resin with dialysis buffer for a 1:1 slurry composition.

7. Run 2ul-5ul samples on 10% SDS gel to check for binding.

Process Steps for Preparation of His6-SpireCT520-991+Spire-KIND Lysate/ His-SpireCT699-991+Spire-KIND lysate

1. Re-suspend 2ml of packed cells with 8ml of 1xPBS.

2. Microfluidize cells and add 10% TritonX100 to cell lysate to make it 0.5% TritonX100; rotate for 30 minutes at 4 °C.

3. Centrifuge at 20,000g for 20 minutes at 4 °C; transfer supernatant to a new tube.

4. Measure OD(280) and dilute with 1xPBS to a final concentration of 2mg/ml; Absorbance of one unit will give rough estimate of 1mg/ml for protein concentration.

GST-Rab Pulldown of His6-SpireCT520-991+Spire-KIND/His-SpireCT699-991+Spire-KIND

1. Wash 30ul of GST-Rab resin with pulldown buffer; discard supernatant and wash in 1xPBS a few times. Remove sup and go to next step.

2. Add 1ml of protein supernatant to the tube of GST-Rab resin; rotate for 1 hour at 4 °C.

3. Wash resin 3 times (1000rpm for 1 minute) with cold 1xPBS.

4. Re-suspend resin in 100ul 1xPBS buffer and take sample to run on 10% protein gel.

5. Run negative control with just GST resin and Spire constructs.

2.11 Western Blot Protocol

After running protein gel, prepare the following material for western protein transfer: Two sponge layers, two Whatman filter paper layers (cut to the size of the sponges), and one PVDF Li-COR membrane. Activate PVDF membrane by soaking it in tray containing methanol. In a separate tray, soak the filter paper and sponge layers in transfer buffer (1L: 10% Methanol, 50ml of 10X Running Buffer (30g Tris Base, 144g Glycine)/1L, 1ml of 10% SDS; Rest fill with ddH_2O). Now assemble the Western sandwich in this order: Black side, sponge, filter paper, protein gel, PVDF membrane, filter paper, sponge, Clear side. Between each layering, smooth out the setup to make sure there are no bubbles in the assembly. Insert Western sandwich into gel box along with an ice pack. Add in the transfer buffer and run at 100V for 3 hours while in an ice bucket.

Dissemble Western apparatus after completion and incubate in blocking buffer (1xTBS (150mM NaCl, 10mM Tris, pH 8.0), 0.05% v/v Tween-20, 3% m/v BSA) for 1 hour at room temperature or overnight at 4°C. After blocking, incubate membrane with desired primary antibody in blocking buffer: Mouse anti-His6 1:10000 dilution, Mouse anti-GFP 1:2000 dilution. Incubate overnight at 4°C. Wash the membrane with 1xTBST (1xTBS+0.2% Tween-20) for 5 minutes and repeat for three times. Incubate with secondary antibody diluted into blocking buffer. Perform same wash steps with 1xTBST and proceed to image western membrane on Li-COR.

2.12 *Drosophila* MiMIC system

Various types of transposons have been used to alter the *Drosophila* genome and to characterize the function of specific genes of interests. Minos-mediated integration cassette (MiMIC) is a Minos transposon carrying a dominant marker along with a gene-trap cassette positioned between two inverted phiC31 integrase attP sites. The sequence between attP sites can be replaced with any other sequence through the action of recombinase-mediated cassette exchange (RCME). The dominant marker in the gene-trap cassette serves as a selection marker for successful MiMIC insertion. In a 2011 paper by Venken et al, the group included the yellow+, a dominant body-color marker, into the gene cassette. With successful insertion, the yellow+ marker would no longer be present in the fly line and thus one can select for non-yellow+ flies for the specific MiMIC insertion.

2.13 Fly Cross Schematic Introduction of GAL4 into Spire promoter

We used the MiMIC system in order to obtain a fly line containing a GAL4 driver under the endogenous Spire promoter.

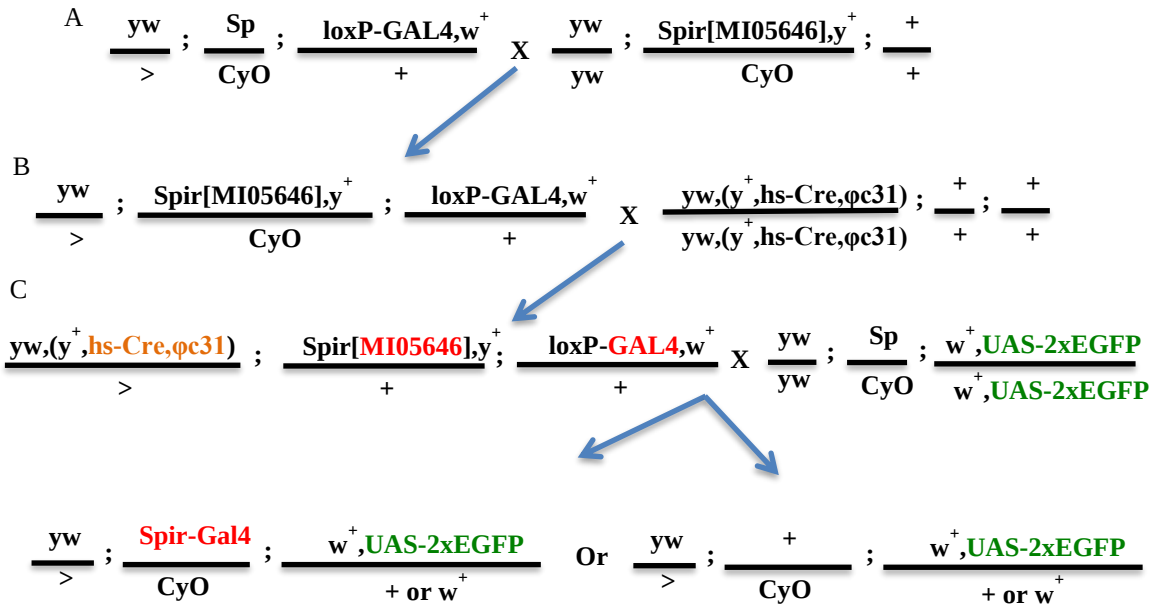

Figure 6: The following crosses were performed in an attempt to obtain a fly line expressing GAL4 driver under the endogenous Spire promoter. As a part of the MiMIC system, the Cre enzyme (orange) was used to insert the GAL4 sequence (red) into the MiMIC site (MI05646 in red). The UAS-2xEGFP (green) reporter was used to differentiate between flies with successful and unsuccessful insertion of GAL4.

Chapter 3: Results

3.1 Truncation of loop sequence in Spire's mFYVE domain

The C-terminus of Spire is shown in Fig. 7B depicting both the Spir-box labeled S and the modified FYVE domain. We deleted a portion of the FYVE domain from SpireCT to generate the SpireCTΔloop construct. Using alignment data with other known FYVE domain proteins, we truncated an unstructured region spanning from residue 814 to residue 949. The alignment data between mammalian and *Drosophila* Spire constructs shows an exclusive 112 amino acid region present between positions 828 and 939 in *Drosophila* Spire (Fig. 7A). We hypothesized that this region was responsible for the aggregation of SpireCT during its purification. Thus, after deleting the unstructured region within the mFYVE domain, we hoped to enhance the solubility of SpireCTΔloop. We designed primers, shown by the blue arrows, to remove the sequence shown in bold in Fig. 7B. Linear PCR product containing all but the loop region of SpireCT was generated and subsequent circularization yielded SpireCTΔloop in a pGEX vector with an N-terminal GST tag. This plasmid was then transformed into bacterial expression cells for its purification.

A

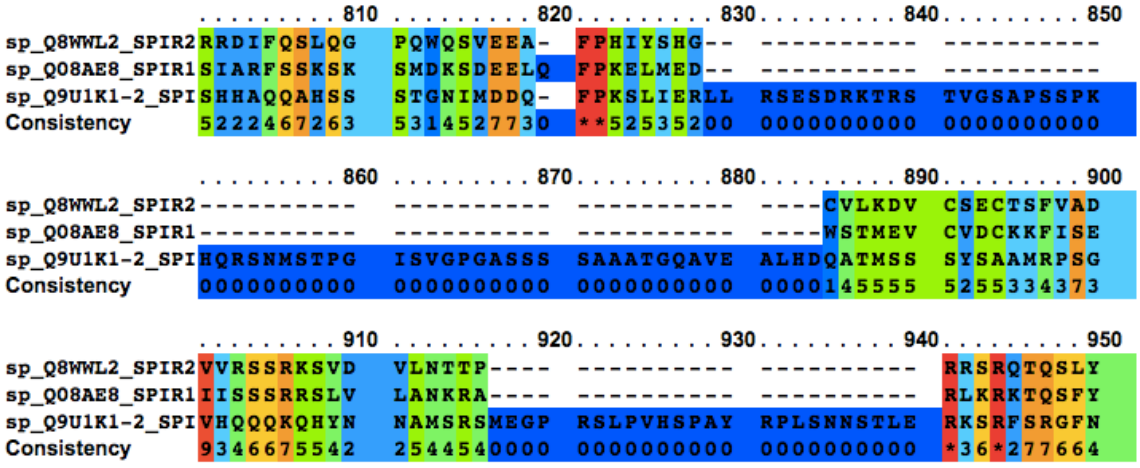

B

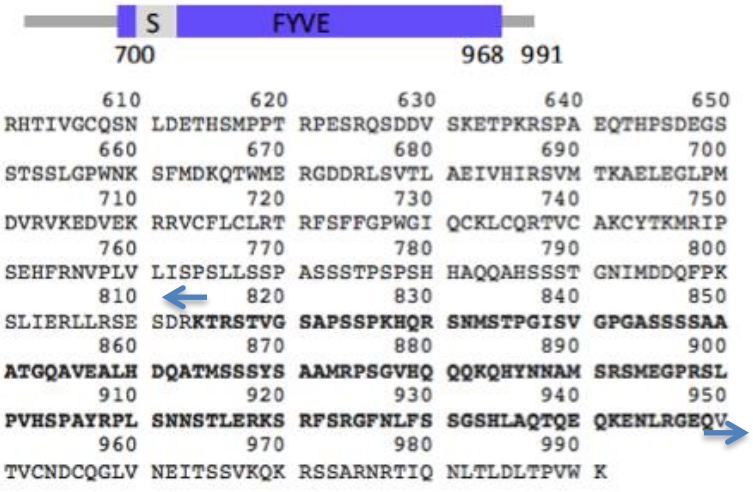

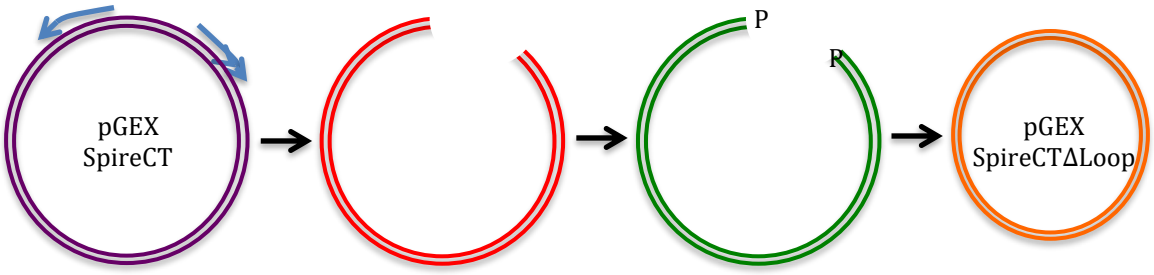

Figure 7: **A)**. Alignment data of Human Spire2 (Spir2), Human Spire1 (Spir1) and *Drosophila* Spire (SPI) above shows the residues of the FYVE and mFYVE domains. The region of non-conversed residues for *Drosophila* Spire extends from around residue 830 through 940. Consistency scale of 0-10 (least conserved to most conserved).
B). SpireCT is depicted in its domain form showing both the Spir-box in gray and the mFYVE domain in blue. The bolded part of the sequence represents the truncated portion of SpireCT. The 136 amino acid truncation spanned from residue 814 to residue 949. The cloning schematic shows the blunt end ligation technique used to generate the GST-SpireCTΔLoop construct. Forward and reverse primers represented by the blue arrows were designed for the sequences adjacent to the truncated region. Subsequent PCR amplification followed by phosphorylation of the 3' ends and blunt end ligation yielded the SpireCTΔLoop construct.

3.2 Soluble GST-SpireCTΔloop does not bind Glutathione Sepharose Resin

We assessed the solubility of GST-SpireCTΔloop through purification attempts. The post-IPTG induction lane showed the enhanced expression of GST-SpireCTΔloop depicted by the red arrow in Fig. 8. After separating the lysed cellular extract through centrifugation, we observed appreciable amounts of GST-SpireCTΔloop in both the supernatant and the cellular debris fraction (pellet) lanes in the 10% SDS gel. The enrichment of GST-SpireCTΔloop in the supernatant, compared to the amount of GST-SpireCT in the supernatant of its purification (gel data not shown), suggests that with the deleted region of the mFYVE domain, the GST-SpireCTΔloop construct was now more soluble than GST-SpireCT. However, the GST-SpireCTΔloop construct did not effectively bind to the Glutathione Sepharose Resin. Much of the protein was lost in the flow through fraction highlighted by the red box in Fig. 8. The elution fraction contained minimal amounts of GST-SpireCTΔloop along with substantial impurities. Purifications were

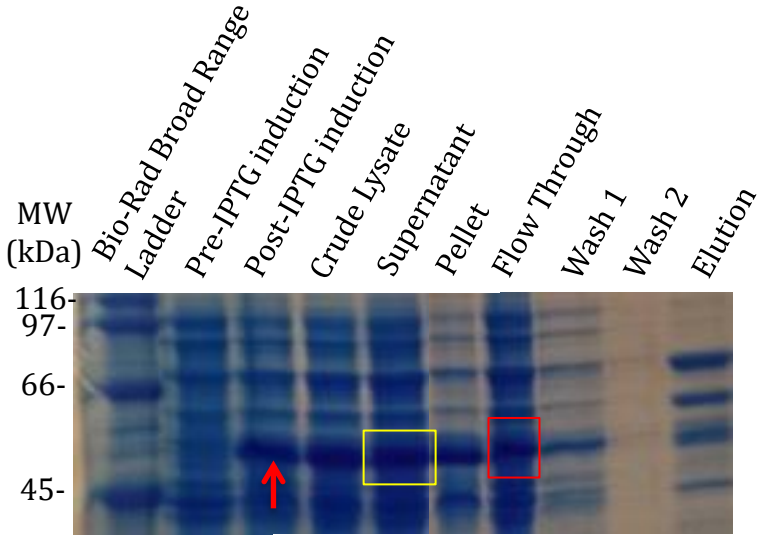

Figure 8: The post-IPTG induction reflects substantial GST-SpireCTΔloop expression over the pre-IPTG induction. Purification of GST-SpireCTΔloop shows soluble protein in the supernatant fractions indicated by the yellow box. This band corresponds to GST-SpireCTΔloop with a molecular weight of 56kDa. Considerable amounts were lost in the flow through fraction shown in the red box.

repeated using different pH and salt concentrations in the extraction buffer and yielded similar results of poor resin binding. Therefore, we sought to use a different affinity tag in an attempt to resolve this issue.

3.3 Purification attempt of His6-SpireCTΔloop

After generating the His6-SpireCTΔloop construct, we employed a similar purification protocol to assess both the solubility of His6-SpireCTΔloop and binding efficiency of the His6 tag to a cobalt metal affinity resin. Similar to the GST-SpireCTΔloop purification, the His6-SpireCTΔloop construct was well expressed and likely soluble as shown by the red arrow in Fig. 9. The appearance of a second band indicated by the orange arrow suggests a nonspecific induction of a protein of similar molecular weight. However, like the GST-SpireCTΔloop construct, the His6 did not improve the binding to the cobalt resin.

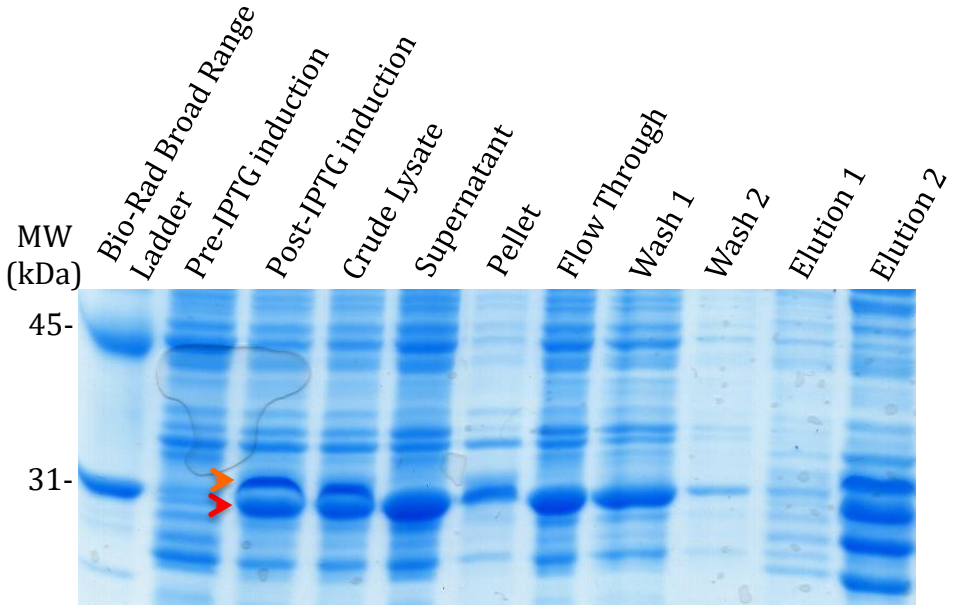

Figure 9: A 10% SDS Gel of the purification of His6-SpireCTΔloop shows soluble protein in the supernatant fraction corresponding to His6-SpireCTΔloop with a molecular weight of 28.36kDa as shown by the red arrow. However, the appearance of a doublet in the induction lane shown by the orange arrow suggests the overexpression of a protein impurity. A substantial amount of His6-SpireCTΔloop was lost in the flow through fraction.

A substantial amount of His6-SpireCTΔloop was lost in the flow through and wash fractions, while only

minimal amounts were retained in the elution fraction. This suggested the possibility that the N-terminus of SpireCTΔloop was structured in such a way that hindered the N-terminal affinity tags from binding to their respective resin columns. Since the His6 tag was directly adjacent to the start of the SpireCTΔloop sequence, we made a final attempt to insert a linker sequence between the His6 tag and the SpireCTΔloop construct. This created distance between the affinity tag and SpireCTΔloop in an effort to possibly mitigate any structural hindrance from the N-terminus of SpireCTΔloop onto the His6 tag.

3.4 Purification attempt of His6-PP-SpireCTΔloop

From His6-SpireCTΔloop, we inserted a 13 amino acid linker between the affinity tag and the beginning of the SpireCTΔloop sequence. This linker also contained a protease cleavage site, which would allow for removal of the His6 tag from the SpireCTΔloop construct. Once again, the purification of His6-PPsite-SpireCTΔloop yielded similar results as the His6-SpireCTΔloop purification. It expressed well and was soluble in the supernatant fraction indicated by the red arrow, but did not bind to the cobalt resin. The majority of His6-PP-SpireCTΔloop was lost in the flow through fraction and the subsequent wash steps. Little to no His6-PP-SpireCTΔloop was observed in the elution fractions (Fig. 10). This further supported the idea that the N-terminus of SpireCTΔloop somehow structurally hinders the accessibility of the affinity tags for the resin and thus affects the binding efficiency of this interaction. Once again, the appearance of the doublet band shown by the orange arrow suggests a possible non-specific overexpression of an off-target protein.

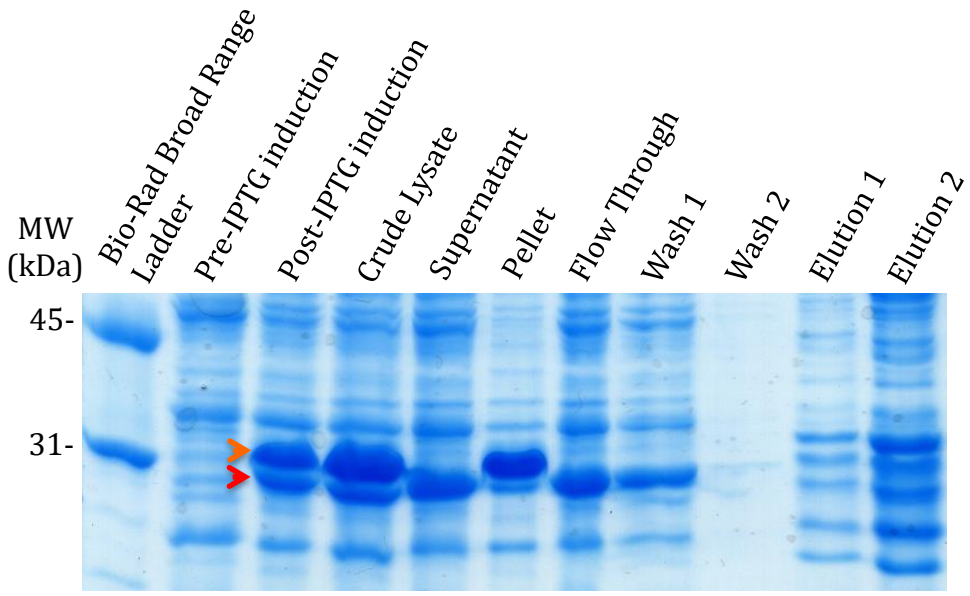

Figure 10: A 10% SDS Gel of the purification of His6-PP-SpireCTΔloop (containing a precision protease linker site between His6 tag and SpireCTΔloop construct) shows soluble His6-PP-SpireCTΔloop in the supernatant fraction corresponding to a molecular weight of 29.72kDa. A considerable amount of His6-PP-SpireCTΔloop was lost in the flow through and wash fractions, while minimally retained in the elution fractions.

3.5 Denatured His6-SpireCTΔloop and His6-PP-SpireCTΔloop bind Talon resin

To understand why the His6 tag was not binding to the cobalt resin, we performed the purification protocol for both His6-PP-SpireCTΔloop and His6-SpireCTΔloop under denaturing conditions using 8M urea in the extraction buffer. If the accessibility of the His6 tag for the cobalt resin was structurally hindered by the N-terminus of the SpireCTΔloop, then by denaturing the construct, it should effectively relieve this hindrance and allow for the His6 tag to bind to the resin. That is what we observed for both His6-PP-SpireCTΔloop and His6-SpireCTΔloop as shown by the red arrows in Fig. 11. When comparing the elution fractions in Fig. 11 against the elution profiles in Fig. 9 and 10, the amount of both His6-PP-SpireCTΔloop and His6-SpireCTΔloop increased significantly. This substantiated the hypothesis that the

N-terminus of SpireCTΔloop was structurally affecting the binding efficiency between the N-terminal affinity tags and their respective resin.

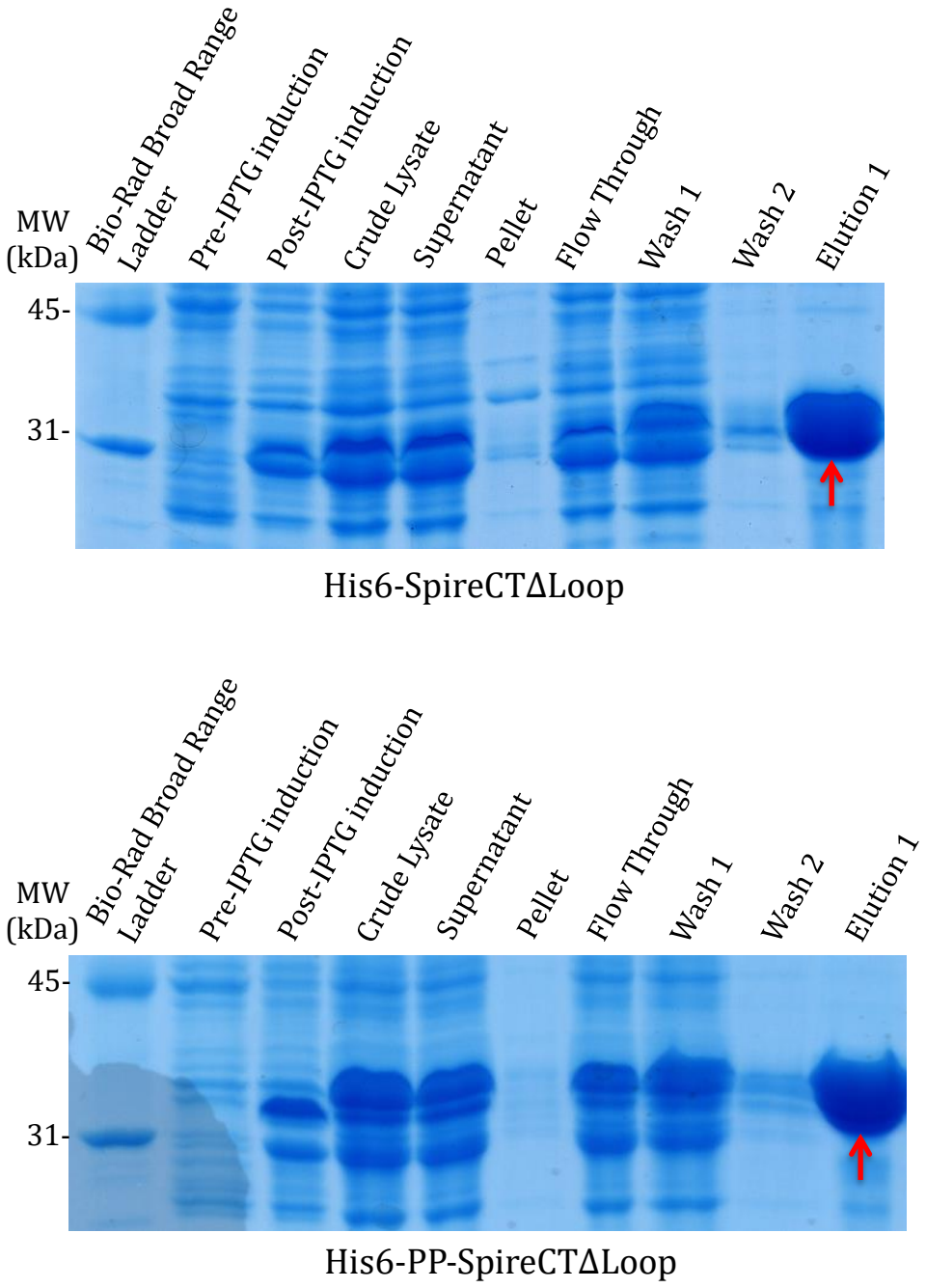

Figure 11: (Top) Purification of His6-SpireCTΔloop under denaturing conditions run on a 10% SDS Gel. The elution fraction showed substantial increase of His6-SpireCTΔloop compared to elution profile in Fig. 9.
(Bottom) A 10% SDS Gel of the purification of His6-PP-SpireCTΔloop under denaturing conditions showed substantial increase of His6-PP-SpireCTΔloop in the elution fraction compared to elution fractions in Fig. 10.

3.6 Refolding attempts of denatured His6-SpireCTΔloop and His6-PP-SpireCTΔloop

Under denaturing conditions, we could isolate relatively pure denatured His6-PPsite-SpireCTΔloop and His6-SpireCTΔloop protein. Thus, we attempted to refold both His6-PPsite-SpireCTΔloop and His6-SpireCTΔloop using dialysis to slowly remove the urea in hopes that both constructs would refold. As shown in Fig. 12, the supernatant fractions after a post-dialysis high-speed centrifugation spin showed minimal amounts of His6-PPsite-SpireCTΔloop and His6-SpireCTΔloop presumably in the refolded state. Most of the protein was in the pellet fraction after the high-speed spin, which indicated that the majority of the protein was aggregated and thus not folded in the correct native structure.

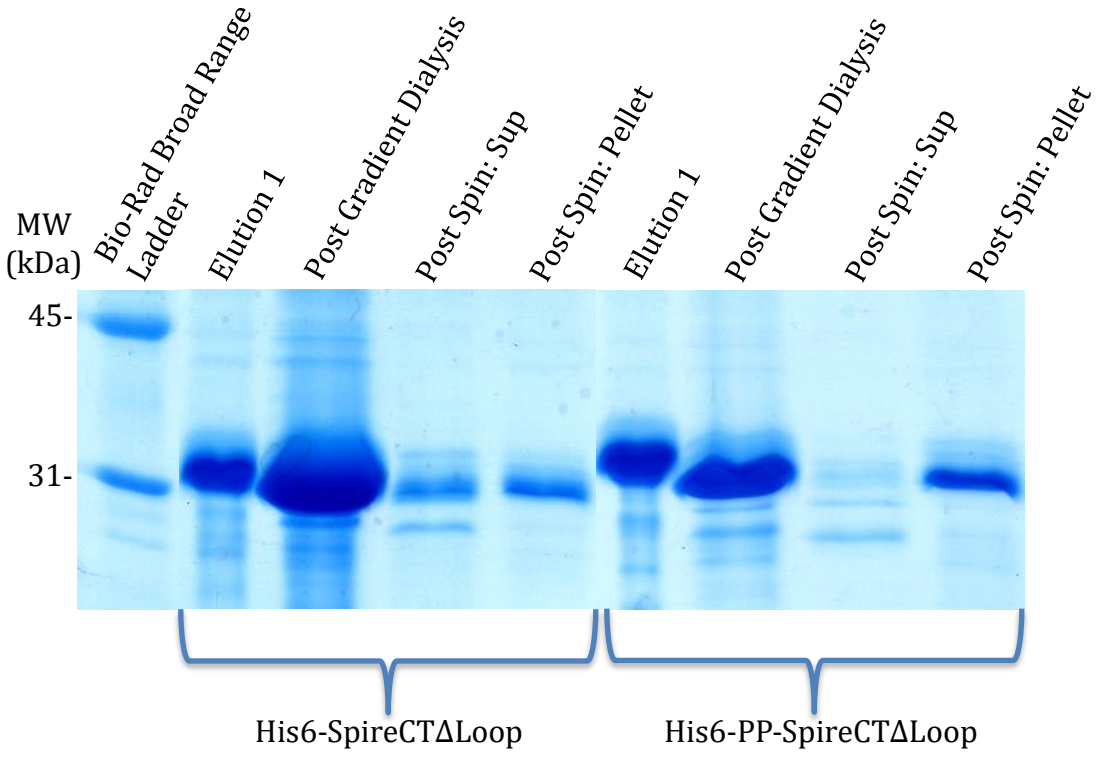

Figure 12: A 10% SDS Gel showing refolding assay of denatured His6-SpirCTΔloop and His6-PP-SpirCTΔloop. The refolding assay was done using dialysis to reduce urea concentration and stimulate protein refolding.

3.7 Co-expression of Spire520-991 and Spire699-991 with Spire-KIND

In our continued efforts to obtain soluble fractions of SpireCT constructs of Spire699-991 and Spire520-991, we co-expressed each construct with Spire-KIND to improve solubility through the intra-molecular binding interaction between the two halves of Spire. We first ran an expression assay comparing the relative levels of the SpireCT constructs when they are singly expressed and when they are co-expressed with Spire-KIND. Both constructs have an N-terminal His6 tag in their respective pET expression vector, so we were able to image them using a primary mouse His6 antibody. Spire-KIND has a native His6 region in its protein sequence, thus also being visualized in the western blot. For both Spire699-991 co-expressed with Spire-KIND and Spire520-991 co-expressed with Spire-KIND, the relative yields of Spire699-991 and Spire520-991 are comparable to when they are singly expressed. This showed that the introduction of a second plasmid for the expression of Spire-KIND did not affect the overall expression levels of the SpireCT constructs indicating that this method was sufficient to maintain the expression level and elevate the soluble fractions of both Spire520-991 and Spire699-991 (Fig. 13).

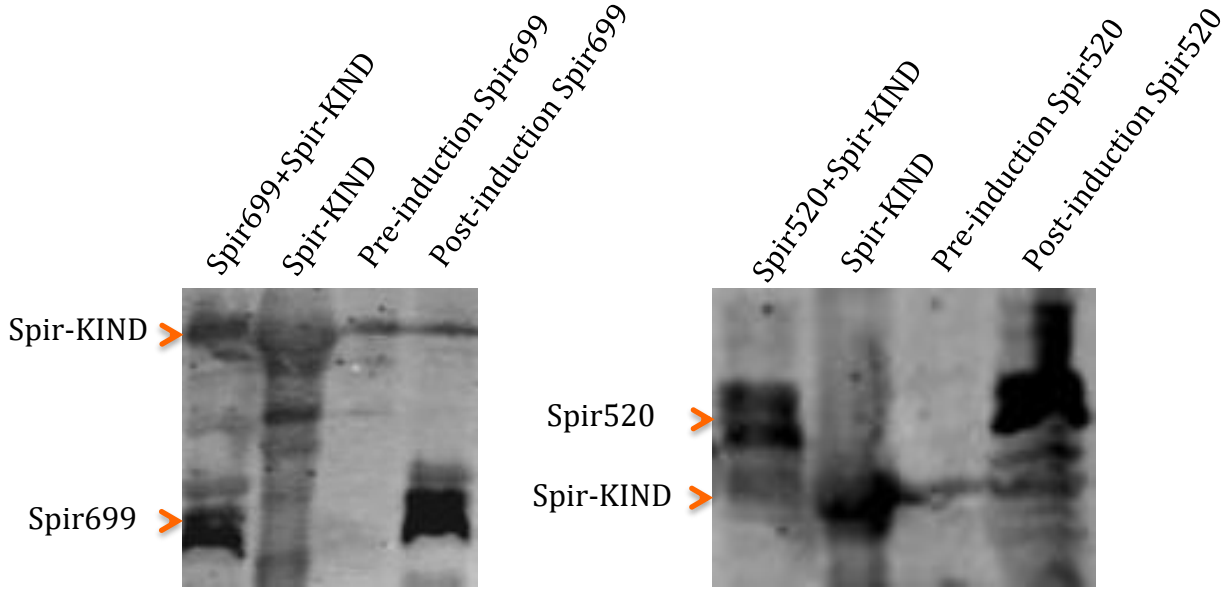

Figure 13: Western blot showing the co-expression assay of Spire699-991+Spire-KIND and Spire520-991+Spire-KIND. The relative levels of Spire520-991 and Spire699-991, when singly and co-expressed, show that the introduction of Spire-KIND had minimal effects on the expression levels of Spire699-991 and Spire520-991.

3.8 Soluble Spire520-991 and Spire699-991 when co-expressed with Spire-KIND

After the overall expression levels of Spire520-991 and Spire699-991 when co-expressed with Spire-KIND were assessed in an expression assay, we next wanted to evaluate the solubility of these two constructs. We ran samples of lysed cell lysate, the supernatant fraction, and the pellet fraction containing the remaining cellular debris, which were separated via a high-speed centrifuge spin. As shown in a western blot probing for the His6 tag, we observed the presence of soluble Spire699 and Spire520 in the supernatant fractions (Fig. 14). A larger fraction of Spire699 was in the soluble form when compared against the soluble portion of Spire520. In both cases, we had sufficient amounts of protein to proceed to the downstream GST-Rab pulldown assay.

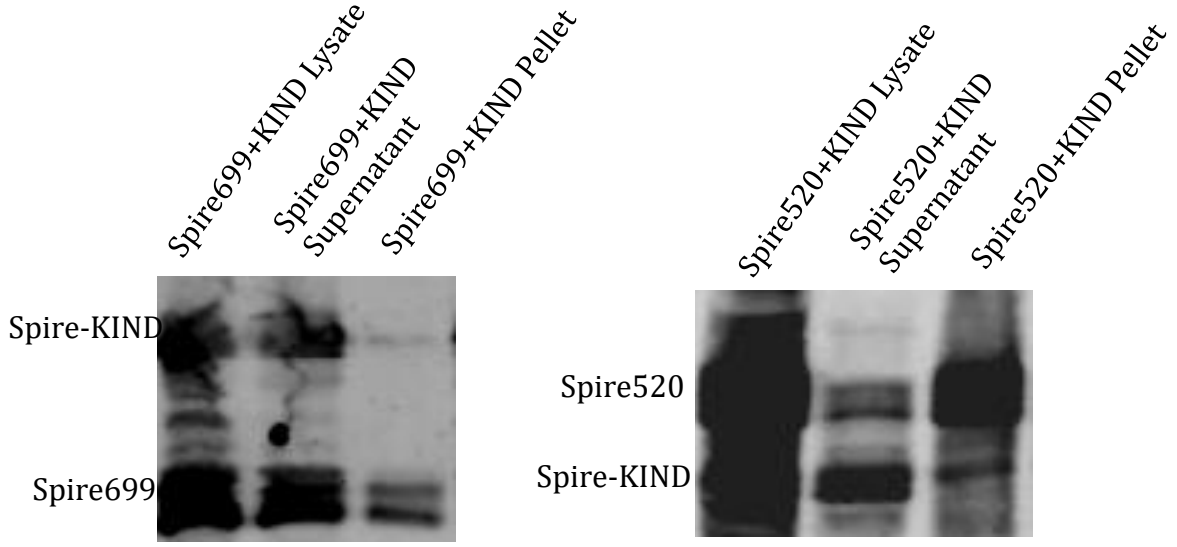

Figure 14: Western blots showing the co-expression of Spire520-991+Spire-KIND and Spire699-991+Spire-KIND. A mouse His6 primary was used to probe for Spire699 and Spire520 as both had N-terminal His6 tags as a part of their pET expression vector. Spire-KIND contains an internal His6 sequence and thus was also visualized. The presence of soluble fractions of Spire699 and Spire520 in the supernatant fractions indicated that the intra-molecular interaction between Spire-KIND and the SpireCT constructs stimulated solubility of a fraction of the protein population as some did remain in the insoluble pellet fraction.

3.9 Purification of GST-Rab5, GST-Rab6, and GST-Rab11 and Preparation for GST-Rab Pulldown Assay

After generating the individual GST-Rab constructs using traditional subcloning techniques, we purified all three constructs following the GST-tagged protein purification schematic as outlined in the methods section. Shown in Fig. 15 is the GST-Rab5 purification with the important samples run on a 10% SDS Gel. The elution profile clearly indicates an abundance of GST-Rab5 that was obtained for later use in the GST-Rab pulldowns. The purification of GST-Rab6 and GST-Rab11 are not shown below, as Fig.

15 is a good representation of the purification outcome of both GST-Rab6 and GST-Rab11. Both purified easily and yielded an abundant amount.

Preparation of the GST-Rab resin for the GST-Rab pulldown assays is shown in the lower 10% SDS Gel in Fig. 15. Purified GST-Rab5, GST-Rab6 and GST-Rab11 were bound to new Glutathione Sepharose Resin for one hour and the resin was assessed for the presence of each Rab construct. As shown in the gel, the lanes for each resin lane contained a sufficient amount of each GST-Rab protein. A negative control of Glutathione Sepharose Resin bound to just GST is also shown in the gel.

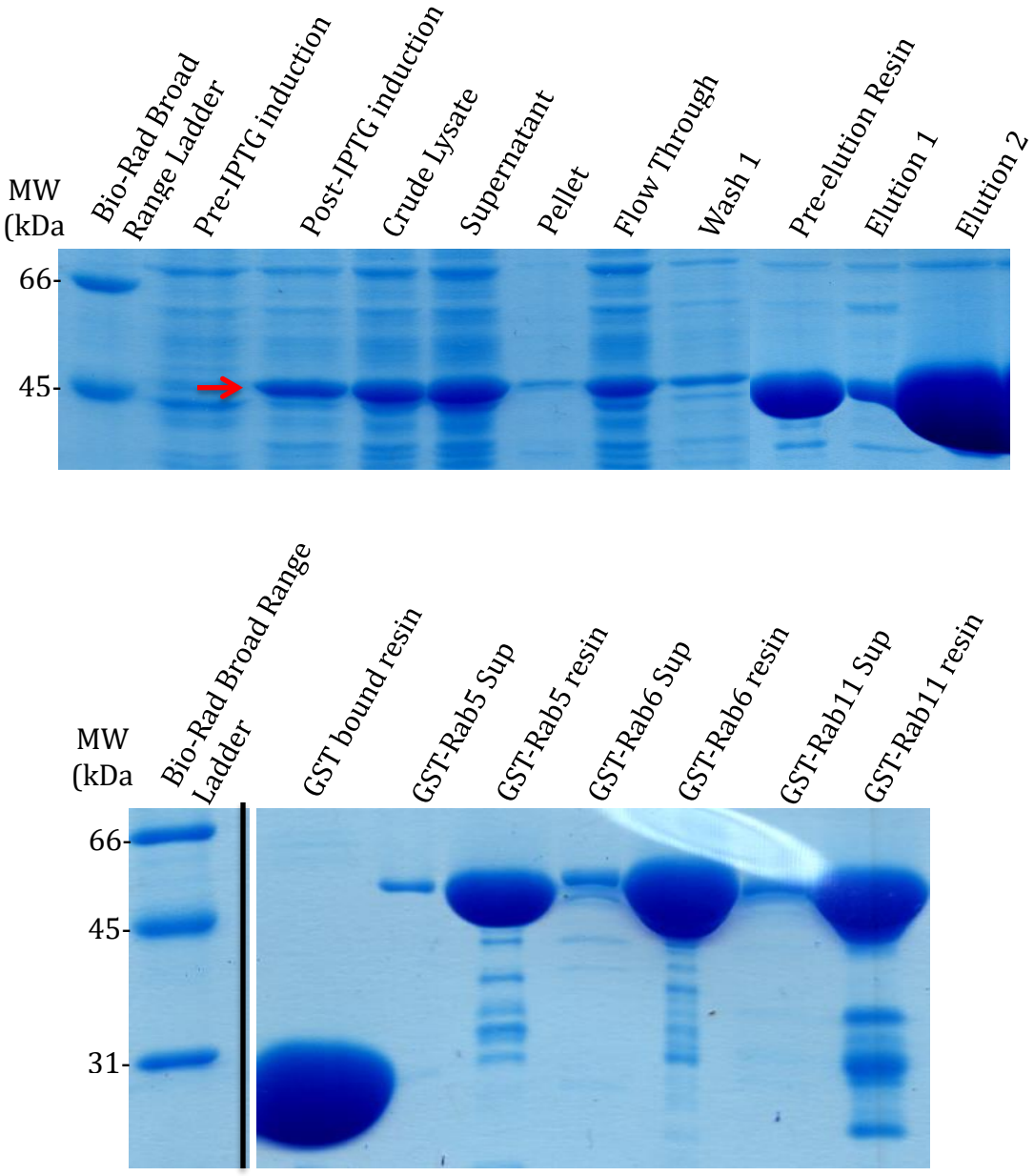

Figure 15:(Top) A 10% SDS Gel showing the purification of GST-Rab5. The majority of the protein was soluble indicated by the red arrow for GST-Rab5 at the molecular weight of 52 kDa. GST-Rab5 was obtained in great quantity in the elution fractions. Only the purification gel for GST-Rab5 is shown here as a reference for the other two GST-Rabs. Both GST-Rab6 and GST-Rab11 were purified in the same manner as GST-Rab5. Their purification gels follow the same trend as the gel for GST-Rab5. (Bottom): A 10% SDS Gel verifying the successful preparation of GST-resin samples for downstream GST-Rab pulldown assay. Each GST-resin lane contained ample amounts of GST, GST-Rab5, GST-Rab6, and GST-Rab11 respectively. The black line denotes lanes not included in the image.

3.10 GST-Rab Pulldown Assay

GST-Rab pulldown assays were performed using Glutathione Sepharose Resin bound to GST, GST-Rab5, GST-Rab6, and GST-Rab11. Negative controls of GST-bound resin and resin only fractions were also used. Samples were incubated with Spire520+Spire-KIND and Spire699+Spire-KIND. Samples of resin from each GST-Rab fraction were collected and analyzed by Western to assess the binding interaction between Spire520 and Spire699 for each of the GST-Rab samples. The Western blots were probed with an anti-His6 antibody for visualization of Spire520, Spire699 and Spire-KIND. Resin samples for each condition were normalized and equal volumes were loaded for comparison between the negative controls and the GST-Rab resins. In comparing the negative controls with the GST-Rab resins, the absence of enrichment of Spire520 and Spire699 in the GST-Rab resins over the negative controls suggests a lack of direct interaction between Spire520 and GST-Rab5, 6,11 as well as between Spire699 and GST-Rab5, 6,11 (Fig. 16).

The experiment was repeated and the same results were reached each time. In this particular Western, the absence of both Spire-KIND and Spire699 for GST-Rab11 is rather odd as previous pulldown repeats yielded fractions of both proteins in the GST-Rab11 lane. Accounting for this, it seems that the complexes of Spire-KIND+Spire520 and Spire-KIND+Spire699 are non-specifically interacting with the GST and not the Glutathione Sepharose Resin itself. Thus, the presence of the complexes in the GST-Rab fractions is likely due to the non-specific interaction with the GST tag on each of the Rab proteins.

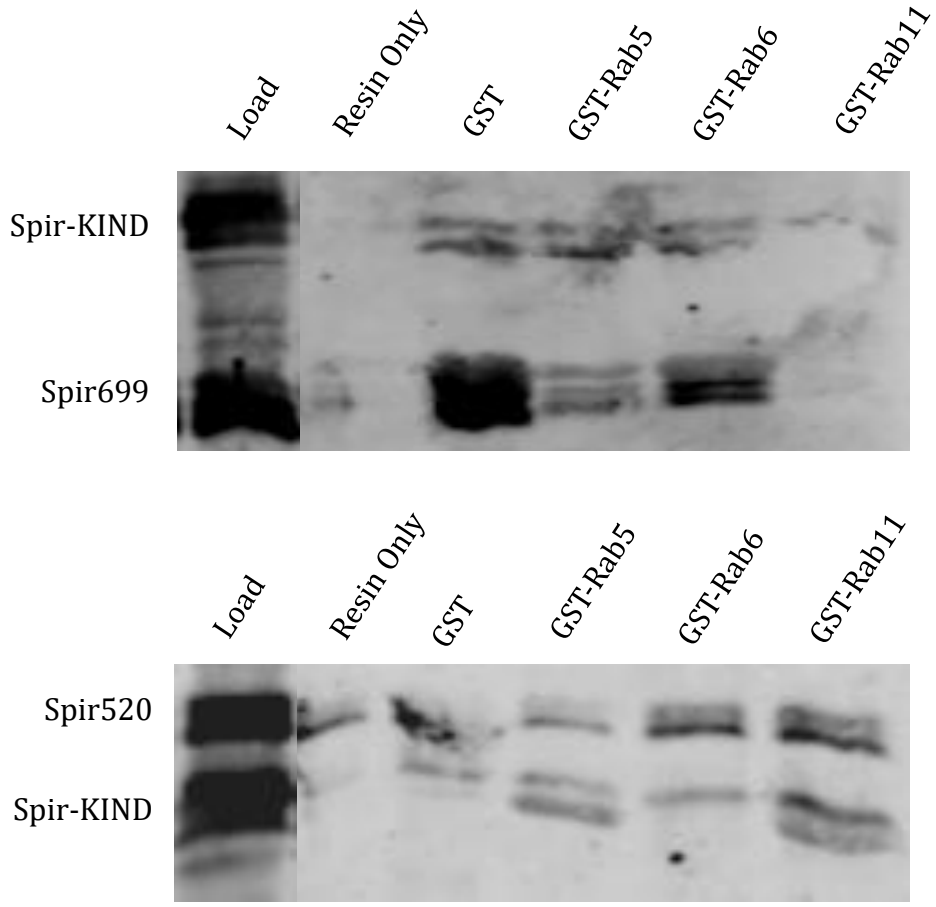

Figure 16: The western blots for the GST-Rab pulldown against Spire699 (top) and Spire520 (bottom) co-expresssed with Spire-KIND. Both Spire699 and Spire-KIND are present as shown in the load fraction. Spire520 and Spire-KIND are also shown in the load fraction. There was no enrichment of Spire699 in the GST-Rab fractions compared to the negative control of GST only. Presence in the negative control reflected non-specific interaction with the GST tag. Spire520 was also not enriched in the GST-Rab fractions compared to the negative control lanes.

.

Chapter Four: Discussion

4.1 SpireCTΔloop

A substantial part of this project focused on improving the solubility of SpireCT as previous recombinantly expressed SpireCT yielded predominantly insoluble aggregates. The first strategy we employed involved the removal of a loop sequence within the mFYVE domain of the SpireCT construct. Membrane domains are often challenging to fold into the proper structural conformation, thus affecting the overall solubility of the protein being expressed recombinantly in E.coli. This loop sequence within the mFYVE domain was thought to affect the folding of SpireCT due to its predicted flexibility and unstructured nature. Through blunt ligation cloning, we deleted the region spanning residues 814 to 949 and generated the new GST- SpireCTΔloop construct. During the purification, this new construct was soluble as opposed to the original SpireCT construct, which aggregated when individually expressed. However, during the purification of GST- SpireCTΔloop, the GST tag of SpireCTΔloop did not effectively bind the resin and the protein was lost in the flow through and wash fractions. Optimization of purification conditions did not improve the binding efficiency of the GST tag. Next, we considered using a different affinity tag in order to mediate the ineffectiveness of the GST tag binding to the Glutathione Sepharose Resin.

For the SpireCTΔloop construct we exchanged the N-terminal GST tag with a His6 tag. Since the GST tag did not bind the Glutathione Sepharose resin, it might not be in the correctly folded state. The His6 tag on the other hand needs only to be accessible to bind to its respective resin thus we opted for the smaller tag in this instance. The purification of His- SpireCTΔloop revealed the same types of issues as the GST- SpireCTΔloop construct. It remained soluble but again was not binding the cobalt resin. This indicated that the N-terminal tags are somehow obstructed from binding to their respective resins.

We then added a linker sequence between the His6 tag and the start of the SpireCTΔloop construct. The motivation being that distance between the tag and the N-terminus of the protein construct could alleviate any structural hindrance that the SpireCTΔloop has on the His6 tag for it not to bind the resin effectively. This new construct His6-PP- SpireCTΔloop also did not bind to the resin.

After conducting the purification protocol on both His6-PP- SpireCTΔloop and His6- SpireCTΔloop constructs under denaturing conditions, we observed the vast increase in protein binding for the resin. This meant that once the protein structure was disrupted the His6 tag was now accessible to bind to the resin. This was verified on an SDS gel shown in Fig. 11. The elution profiles of the denatured purifications contained predominantly the two proteins of interest. This established that indeed the N-terminal portion of SpirCTΔloop structurally blocked the accessibility of the His6 tag to the resin.

One interesting aspect of the expression of both His6-SpireCTΔLoop and His6-PP-SpireCTΔLoop is the presence of a major secondary band that runs very close to the protein of interest. This band is only heavily expressed when induced with IPTG. Thus, it stands to reason that it is also a form of our protein of interest or perhaps a chaperone. However, when we performed MALDI mass spectroscopy on the elution fractions, we observed two predominant species differing in mass by only 2-3 amino acids in each of the samples. Both protein constructs correlated with the species with the heavier mass, which suggests that our protein of interest was the top band of the doublet seen in each of their purification gel. However, the difference of only 2-3 amino acids does not reconcile the distance between the two bands in the SDS-PAGE gel. Furthermore, if our protein of interest is indeed the top band of the doublet, then its solubility did not improve and thus we were apprehensive in moving forward with this strategy.

In addition, we performed a GST-Rab pulldown using His6-SpireCTΔloop lysate and did not observe a strong band for our protein or any particular enrichment in the GST-Rab lanes over the negative controls, which would indicate an interaction between Spire and Rab when visualized on a Western. The loop

deletion might also cause issues in downstream pulldown assays as its proximity to the Spir-box could affect its structure when the loop is truncated.

Given the current status of this strategy, we might revisit the GST-SpireCTΔloop construct since it is not expressed as a doublet as shown in its purification gel. This would mitigate issues of the doublet expression for both His6 constructs. It would also be worthwhile to test the lysate of GST-SpireCTΔloop in a GST-Rab pulldown and observe if there are any significant differences between the GST tagged and His6 tagged SpireCTΔloop constructs in interacting with GST-Rabs.

4.2 Co-expression of SpireCT constructs

Co-expression of Spire699 with Spire-KIND and Spire520 with Spire-KIND did yield soluble fractions of both Spire699 and Spire520. However, we did not succeed in separating them suggesting that for both constructs to remain soluble, they must be associated with Spire-KIND. This would not be an issue if the goal were just to show that they could be solubilized when co-expressed with Spire-KIND. We wanted to take these soluble fractions and conduct downstream biochemical binding assays with them. Having Spire-KIND bound to both Spire699 and Spire520 could affect the binding interaction with Rabs and mask any potential direct interaction between Spire and Rabs. Moving forward, we might try eluting and subjecting the complex to higher salt concentrations to dissociate the two proteins from each other. However, once dissociated, both Spire520 and Spire699 might aggregate again and thus would require the continuous association with Spire-KIND to remain soluble.

4.3 Direct interaction between Spire and Rabs

GST-Rab Pulldown assay using GST-Rab5, GST-Rab6, and GST-Rab11 did not show a direct interaction with Spire520 and Spire699 co-expressed in complex with Spire-KIND. The western blots in

Fig. 15 show the co-expression levels of both Spire699 with Spire-KIND and Spire520 with Spire-KIND. Both Spire699 and Spire520 were present in the soluble fractions. However, incubation of these soluble fractions with GST-Rabs did not show any apparent binding interaction of either Spire520 or Spire699 for the three GST-Rabs. The absence of an interaction with Rab5 substantiates the absence of co-localization between Spire and Rab5 in NIH 3T3 cells. For Rabs 6 and 11, this likely means that there is not a direct interaction between the two Rabs and Spire. However, given that the complexes of Spire-KIND+Spire699 and Spire-KIND+Spire520 both interacts non-specifically with the GST only negative control, it could be possible that this non-specific interaction is masking a possible weak direct interaction with the Rab proteins. In moving forward, we would switch the GST tags on each of the Rab constructs in order to mitigate any nonspecific interactions Spire699 and Spire520 are having with the GST tag. As previously mentioned, Spire-KIND might also be affecting the binding interaction between both Spire520 and Spire699 for the Rabs. If we could dissociate the complexes without compromising the solubility of both Spire699 and Spire520, then we could more directly test for binding interactions between Spire and Rabs.

4.4 Fly Crosses

Fly crosses were successfully performed following the schematic shown in Fig. 6. Progeny from cross C were dissected to visualize EGFP signal driven by Spire-GAL4 to validate successful transposition of GAL4 driver into the endogenous Spire promoter. We did not observe any fluorescence signal and when we performed a control cross between nanos-GAL4 flies with our 2x-EGFP reporter flies, we also did not observe any fluorescence signal. However, florescence signal was detected when nanos-GAL4 flies were crossed with two other GFP reporter fly lines we had in the lab. Lastly, we crossed our 2x-EGFP reporter flies with a non-embryonic GAL4 driver, Fhod-GAL4, and observed bright fluorescence signal. Thus, our 2x-EGFP was not working for germline specific GAL4 drivers. Currently, we are redoing our crosses with

a different GFP reporter line in hopes of obtaining the correct fly with Spire-GAL4 on the second chromosome.

4.5 Future Direction

Given the current results of our pulldown assays, they do not rule out any direct interactions between Rabs and Spire, though they do not favor it.

I am now performing GST-Rab pulldown assays using fly ovary lysate to ask whether an interaction between *Drosophila* Spire and Rab5, Rab6, and Rab11 can be observed, similar to the results of mammalian Rab11 with expressed Spire1 in HEK293 lysate. I am expressing full-length GFP-Spire construct in its endogenous environment, as we do not have a reliable Spire antibody. GFP-Spire is expected to be functional based on previous rescue experiments with Spire null flies (Quinlan, 2013). We can also learn about potentially new binding proteins that could function to mediate the interaction between Spire and Rab GTPases using this approach. A recent crystal structure depicts direct interaction between the globular tail domain of Myosin 5 (GTD) and the region of Spire between the WH2 domains and the Spir-box as well as the GTD bound to Rab11 (Pylypenko et al., 2016). This suggests that the interaction between Spire and Rabs are likely mediated through other protein factors.

References

1. Aivazian, D.; Serrano, R. L.; Pfeffer, S., TIP47 is a key effector for Rab9 localization. *J Cell Biol* **2006,** *173* (6), 917-26.

2. Apodaca, G.; Gallo, L. I.; Bryant, D. M., Role of membrane traffic in the generation of epithelial cell asymmetry. *Nat Cell Biol* **2012,** *14* (12), 1235-43.

3. Cao, X.; Surma, M. A.; Simons, K., Polarized sorting and trafficking in epithelial cells. *Cell Res* **2012,** *22* (5), 793-805.

4. Chan, C. C.; Scoggin, S.; Wang, D.; Cherry, S.; Dembo, T.; Greenberg, B.; Jin, E. J.; Kuey, C.; Lopez, A.; Mehta, S. Q.; Perkins, T. J.; Brankatschk, M.; Rothenfluh, A.; Buszczak, M.; Hiesinger, P. R., Systematic discovery of Rab GTPases with synaptic functions in *Drosophila*. *Curr Biol* **2011,** *21* (20), 1704-15.

5. Colicelli, J., Human RAS superfamily proteins and related GTPases. *Sci STKE* **2004,** *2004* (250), Re13.

6. Coutelis, J. B.; Ephrussi, A., Rab6 mediates membrane organization and determinant localization during *Drosophila* oogenesis. *Development* **2007,***134* (7), 1419-30.

7. Dahlgaard, K.; Raposo, A. A.; Niccoli, T.; St Johnston, D., Capu and Spire assemble a cytoplasmic actin mesh that maintains microtubule organization in the *Drosophila* oocyte. *Dev Cell* **2007,** *13* (4), 539-53.

8. Del Nery, E.; Miserey-Lenkei, S.; Falguieres, T.; Nizak, C.; Johannes, L.; Perez, F.; Goud, B., Rab6A and Rab6A' GTPases play non-overlapping roles in membrane trafficking. *Traffic* **2006,** *7* (4), 394-407.

9. DiAntonio, A.; Burgess, R. W.; Chin, A. C.; Deitcher, D. L.; Scheller, R. H.; Schwarz, T. L., Identification and characterization of *Drosophila* genes for synaptic vesicle proteins. *J Neurosci* **1993,** *13* (11), 4924-35.

10. Dollar, G.; Struckhoff, E.; Michaud, J.; Cohen, R. S., Rab11 polarization of the *Drosophila* oocyte: a novel link between membrane trafficking, microtubule organization, and oskar mRNA localization and translation. *Development* **2002,** *129* (2), 517-26.

11. Dunst, S.; Kazimiers, T.; von Zadow, F.; Jambor, H.; Sagner, A.; Brankatschk, B.; Mahmoud, A.; Spannl, S.; Tomancak, P.; Eaton, S.; Brankatschk, M., Endogenously tagged rab proteins: a resource to study membrane trafficking in *Drosophila*. *Dev Cell* **2015,** *33* (3), 351-65.

12. Emery, G.; Hutterer, A.; Berdnik, D.; Mayer, B.; Wirtz-Peitz, F.; Gaitan, M. G.; Knoblich, J. A., Asymmetric Rab 11 endosomes regulate delta recycling and specify cell fate in the *Drosophila* nervous system. *Cell* **2005,** *122* (5), 763-73.

13. Gorvel, J. P.; Chavrier, P.; Zerial, M.; Gruenberg, J., rab5 controls early endosome fusion in vitro. *Cell* **1991,** *64* (5), 915-25.

14. Holubcova, Z.; Howard, G.; Schuh, M., Vesicles modulate an actin network for asymmetric spindle positioning. *Nat Cell Biol* **2013,** *15* (8), 937-47.

15. Januschke, J.; Nicolas, E.; Compagnon, J.; Formstecher, E.; Goud, B.; Guichet, A., Rab6 and the secretory pathway affect oocyte polarity in *Drosophila*. *Development* **2007,** *134* (19), 3419-25.

16. Johnstone, O.; Lasko, P., Translational regulation and RNA localization in *Drosophila* oocytes and embryos. *Annu Rev Genet* **2001,** *35*, 365-406.

17. Jordens, I.; Marsman, M.; Kuijl, C.; Neefjes, J., Rab proteins, connecting transport and vesicle fusion. *Traffic* **2005,** *6* (12), 1070-7.

18. Kerkhoff, E.; Simpson, J. C.; Leberfinger, C. B.; Otto, I. M.; Doerks, T.; Bork, P.; Rapp, U. R.; Raabe, T.; Pepperkok, R., The Spir actin organizers are involved in vesicle transport processes. *Curr Biol* **2001,** *11* (24), 1963-8.

19. Mallard, F.; Tang, B. L.; Galli, T.; Tenza, D.; Saint-Pol, A.; Yue, X.; Antony, C.; Hong, W.; Goud, B.; Johannes, L., Early/recycling endosomes-to-TGN transport involves two SNARE complexes and a Rab6 isoform. *J Cell Biol* **2002,** *156* (4), 653-64.

20. Manseau, L. J.; Schupbach, T., cappuccino and spire: two unique maternal-effect loci required for both the anteroposterior and dorsoventral patterns of the *Drosophila* embryo. *Genes Dev* **1989,** *3* (9), 1437-52.

21. Martinez, O.; Antony, C.; Pehau-Arnaudet, G.; Berger, E. G.; Salamero, J.; Goud, B., GTP-bound forms of rab6 induce the redistribution of Golgi proteins into the endoplasmic reticulum. *Proc Natl Acad Sci U S A* **1997,** *94* (5), 1828-33.

22. Opdam, F. J.; Echard, A.; Croes, H. J.; van den Hurk, J. A.; van de Vorstenbosch, R. A.; Ginsel, L. A.; Goud, B.; Fransen, J. A., The small GTPase Rab6B, a novel Rab6 subfamily member, is cell-type specifically expressed and localised to the Golgi apparatus. *J Cell Sci* **2000,** *113 (Pt 15)*, 2725-35.

23. Ortiz, D.; Medkova, M.; Walch-Solimena, C.; Novick, P., Ypt32 recruits the Sec4p guanine nucleotide exchange factor, Sec2p, to secretory vesicles; evidence for a Rab cascade in yeast. *J Cell Biol* **2002,** *157* (6), 1005-15.

24. Ostermeier, C.; Brunger, A. T., Structural basis of Rab effector specificity: crystal structure of the small G protein Rab3A complexed with the effector domain of rabphilin-3A. *Cell* **1999,** *96* (3), 363-74.

25. Otto, I. M.; Raabe, T.; Rennefahrt, U. E.; Bork, P.; Rapp, U. R.; Kerkhoff, E., The p150-Spir protein provides a link between c-Jun N-terminal kinase function and actin reorganization. *Curr Biol* **2000,** *10* (6), 345-8.

26. Paunola, E.; Mattila, P. K.; Lappalainen, P., WH2 domain: a small, versatile adapter for actin monomers. *FEBS Lett* **2002,** *513* (1), 92-7.

27. Pavlos, N. J.; Jahn, R., Distinct yet overlapping roles of Rab GTPases on synaptic vesicles. *Small GTPases* **2011,** *2* (2), 77-81.

28. Pfeffer, S. R., Unsolved mysteries in membrane traffic. *Annu Rev Biochem* **2007,** *76*, 629-45.

29. Pollard, T. D.; Borisy, G. G., Cellular motility driven by assembly and disassembly of actin filaments. *Cell* **2003,** *112* (4), 453-65.

30. Purcell, K.; Artavanis-Tsakonas, S., The developmental role of warthog, the notch modifier encoding Drab6. *J Cell Biol* **1999,** *146* (4), 731-40.

31. Pylypenko, O.; Welz, T.; Tittel, J.; Kollmar, M.; Chardon, F.; Malherbe, G.; Weiss, S.; Michel, C. I.; Samol-Wolf, A.; Grasskamp, A. T.; Hume, A.; Goud, B.; Baron, B.; England, P.; Titus, M. A.; Schwille, P.; Weidemann, T.; Houdusse, A.; Kerkhoff, E., Coordinated recruitment of Spir actin nucleators and myosin V motors to Rab11 vesicle membranes. *Elife* **2016,** *5*.

32. Quinlan, M. E.; Heuser, J. E.; Kerkhoff, E.; Mullins, R. D., *Drosophila* Spire is an actin nucleation factor. *Nature* **2005,** *433* (7024), 382-8.

33. Quinlan, M. E.; Hilgert, S.; Bedrossian, A.; Mullins, R. D.; Kerkhoff, E., Regulatory interactions between two actin nucleators, Spire and Cappuccino. *J Cell Biol* **2007,** *179* (1), 117-28.

34. Quinlan, M. E., Direct interaction between two actin nucleators is required in Drosophila oogenesis. *Development* **2013,** *140*(21), 4417-25.

35. Riechmann, V.; Ephrussi, A., Axis formation during *Drosophila* oogenesis. *Curr Opin Genet Dev* **2001,** *11* (4), 374-83.

36. Rivera-Molina, F. E.; Novick, P. J., A Rab GAP cascade defines the boundary between two Rab GTPases on the secretory pathway. *Proc Natl Acad Sci U S A* **2009,** *106* (34), 14408-13.

37. Satoh, A. K.; O'Tousa, J. E.; Ozaki, K.; Ready, D. F., Rab11 mediates post-Golgi trafficking of rhodopsin to the photosensitive apical membrane of *Drosophila* photoreceptors. *Development* **2005,** *132* (7), 1487-97.

38. Schmitt, H. D.; Wagner, P.; Pfaff, E.; Gallwitz, D., The ras-related YPT1 gene product in yeast: a GTP-binding protein that might be involved in microtubule organization. *Cell* **1986,** *47* (3), 401-12.

39. Shetty, K. M.; Kurada, P.; O'Tousa, J. E., Rab6 regulation of rhodopsin transport in *Drosophila*. *J Biol Chem* **1998,** *273* (32), 20425-30.

40. Sonnichsen, B.; De Renzis, S.; Nielsen, E.; Rietdorf, J.; Zerial, M., Distinct membrane domains on endosomes in the recycling pathway visualized by multicolor imaging of Rab4, Rab5, and Rab11. *J Cell Biol* **2000,** *149* (4), 901-14.

41. Stenmark, H., Rab GTPases as coordinators of vesicle traffic. *Nat Rev Mol Cell Biol* **2009,** *10* (8), 513-25.

42. Tanaka, T.; Nakamura, A., The endocytic pathway acts downstream of Oskar in *Drosophila* germ plasm assembly. *Development* **2008,** *135* (6), 1107-17.

43. Tanaka, T.; Nakamura, A., Oskar-induced endocytic activation and actin remodeling for anchorage of the *Drosophila* germ plasm. *Bioarchitecture* **2011,** *1* (3), 122-126.

44. Venken, K. J.; Schulze, K. L.; Haelterman, N. A.; Pan, H.; He, Y.; Evans-Holm, M.; Carlson, J. W.; Levis, R. W.; Spradling, A. C.; Hoskins, R. A.; Bellen, H. J., MiMIC: a highly versatile transposon insertion resource for engineering *Drosophila* melanogaster genes. *Nat Methods* **2011,** *8* (9), 737-43.

45. Vizcarra, C. L.; Kreutz, B.; Rodal, A. A.; Toms, A. V.; Lu, J.; Zheng, W.; Quinlan, M. E.; Eck, M. J., Structure and function of the interacting domains of Spire and Fmn-family formins. *Proc Natl Acad Sci U S A* **2011,** *108* (29), 11884-9.

46. Wellington, A.; Emmons, S.; James, B.; Calley, J.; Grover, M.; Tolias, P.; Manseau, L., Spire contains actin binding domains and is related to ascidian posterior end mark-5. *Development* **1999,** *126* (23), 5267-74.

47. Winter, J. F.; Hopfner, S.; Korn, K.; Farnung, B. O.; Bradshaw, C. R.; Marsico, G.; Volkmer, M.; Habermann, B.; Zerial, M., Caenorhabditis elegans screen reveals role of PAR-5 in RAB-11-recycling endosome positioning and apicobasal cell polarity. *Nat Cell Biol* **2012,** *14* (7), 666-76.

48. Wucherpfennig, T.; Wilsch-Brauninger, M.; Gonzalez-Gaitan, M., Role of *Drosophila* Rab5 during endosomal trafficking at the synapse and evoked neurotransmitter release. *J Cell Biol* **2003,** *161* (3), 609-24.

49. Xu, Y.; Moseley, J. B.; Sagot, I.; Poy, F.; Pellman, D.; Goode, B. L.; Eck, M. J., Crystal structures of a Formin Homology-2 domain reveal a tethered dimer architecture. *Cell* **2004,** *116* (5), 711-23.

50. Zhang, J.; Schulze, K. L.; Hiesinger, P. R.; Suyama, K.; Wang, S.; Fish, M.; Acar, M.; Hoskins, R. A.; Bellen, H. J.; Scott, M. P., Thirty-one flavors of *Drosophila* rab proteins. *Genetics* **2007,** *176* (2), 1307-22.